

Denoising of Radial Bioimpedance Signals using Adaptive Wavelet Packet Transform and Kalman Filter

Pranali C. Choudhari¹, Dr. M. S. Panse²

¹(Department of Electrical Engineering, V.J.T.I., Mumbai, India)

Abstract: In recent years, the accurate computer aided diagnosis of the cardiovascular diseases is gaining momentum. In addition to accuracy, non-invasiveness of the measurement techniques has become the need of the hour. Impedance cardiography is one such method which has become a synonym for indirect assessment of monitoring the stroke volume, cardiac output and other hemodynamic parameters by monitoring the blood volume changes of the body. Changes occurring in the blood volume within a certain body segment due to various physiological processes are captured in terms of the impedance variations of that segment. But this method is affected by electrical noise such as power line hum and motion and respiratory artifacts due to movement of the subject while acquiring the bioimpedance signal. This can cause errors in the automatic extraction of the characteristic points for estimation the hemodynamic parameters. This paper presents two algorithms for baseline wander removal from the bioimpedance waveform obtained at the radial pulse of the left hand, one based on wavelet packet decomposition and the other based on the Kalman filter. The impedance signals have been acquired by using the peripheral pulse analyzer. The results for the wavelet packet decomposition are found to be better than that of the Kalman filter.

Keywords: Bioimpedance, Artifact, Baseline wander, Energy, Impedance cardiography, Radial, Wavelet packet transform, Kalman filter .

I. Introduction

Impedance Cardiography (ICG) is a simple, inexpensive and noninvasive method to monitor electrical impedance change of thorax which is caused by periodic change of blood volume in aorta. An appropriate thorax model can be used for estimating Stroke Volume (SV), Cardiac Output (CO) and other hemodynamic parameters [1]. Electrical bioimpedance uses electric current stimulation for identification of thoracic or body impedance variations induced by cyclic changes in blood flow caused by the heart beating. Cardiac output is continuously estimated using skin electrodes by analyzing the occurring signal variation with different mathematical models. Respiratory and motion artifacts cause baseline drift in the sensed impedance waveform, particularly during or after exercise, and this drift results in errors in the estimation of the parameters [2], [3]. Ensemble averaging [3], a classical statistical technique for baseline cancellation, can be used to suppress the artifacts, but it may blur the characteristics of the waveform which are less distinct, thereby resulting in error in the estimation.

Baseline removal has been addressed in many different ways in literature. In [4], baseline is estimated using the polynomial approximations and then subtracted from the original raw ECG signal. This is a nonlinear method, and its performance is based on estimation of reference points in the PR intervals. The main disadvantage of this method is estimating reference points that may not belong to baseline. In [5], a linear time-varying filtering approach is undertaken to suppress the baseline drift in the ECG signal. Low-pass filtering is applied to estimate the baseline wander and is interpolated. Then it is subtracted from the original signal. This is a nonlinear approach so it is complex and highly dependent to beat rate calculations and becomes less accurate in low heart rates. Using the linear filtering approach a digital narrow-band linear-phase filter with cut-off frequency of 0.8 Hz has been suggested in [6]. Another filtering technique using digital and hybrid linear-phase with cut-off frequency of 0.64 Hz is used in [7]. Though the method looks quite simple to implement, the number of coefficients used the FIR structure is too high and resulting long impulse responses. Since there is an overlap on the spectrums of the baseline and the bioimpedance signals, removing baseline spectrum will cause distortion on the signal components. Time-varying filtering was proposed in [4]. Filter banks with different cut-off frequencies which depend on heart rate and baseline level was implemented. Due to a partial overlap between the spectra of ICG and the artifacts, non-adaptive digital filters have not been reported to be effective in removing the artifacts.

A typical ICG waveform measured across the thorax of the human body and its characteristic points is shown in Fig. 1. Points B, C and X are the three main characteristic of ICG trace. Point B represents opening of the aortic valve, while point X denotes closing of the aortic valve. The point Z corresponds to peak of the ICG waveform, while the point X is the lowest point in the ICG waveform. The time interval between point B and

point X is the Left Ventricle Ejection Time (LVET) [8]. SV is generally calculated using Kubicek's equation using two hemodynamic parameters: the LVET and the dz/dt_{max} of ICG [9].

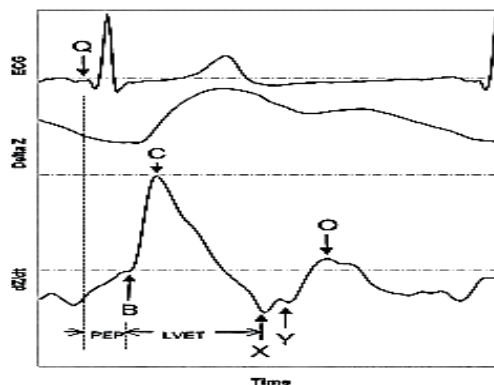


Figure 1: ICG and ECG signals

There are two major artifacts in the ICG signal: respiratory and motion artifacts. Respiratory artifacts have very low frequency (0.04-2 Hz), and the frequency of motion artifacts is about 0.1-10 Hz. The baseline drift is due to the respiratory artifacts, while the peaks variation is due to motion artifacts. ICG signal range is 0.8 to 20 Hz, therefore respiratory and motion artifacts lie within the same band [10]. The electrical impedance change caused by blood volume change in aorta typically accounts for 2-4% of the base impedance (usually about 20ohm), while the electrical impedance change caused by the respiratory artifact and motion artifact may be 30% or even more [9]. Therefore the motion and respiratory artifacts may lead to a large baseline drift in the ICG signal, subsequently resulting in errors in extraction of the characteristic points and calculation of the hemodynamic parameters. ICG signal is modulated by breath which can cause its fluctuation around base impedance Z_0 , thus baseline drift is inevitable during exercise. Subsequently baseline drift might cause inaccurate calculations of hemodynamic parameters when the zero level is used to calculate dz/dt_{max} . Therefore removing respiratory artifact from ICG signal is really important. Moreover, the noise sources such as power line hum, change in impedance of the electrodes due to perspiration also may cause the baseline drift.

The bioimpedance signals used in this paper for suppression of artifacts are obtained by applying the current to the wrist of the left hand instead of the thorax. Due to the smaller diameters of the blood carrying vessels in this region, the amount of the blood volume change and therefore the impedance changes are small. Application of electrodes at this site makes the measurement procedure easy, faster and less traumatic for the patient. Due to smaller amplitudes of the desired signals, removal of baseline wander becomes more challenging. The amplitudes of the desired signal and noise become comparable to each other. Thus the baseline wander removal algorithm should not only eliminate the baseline drift, but also preserve the spectral and temporal characteristics of the bioimpedance waveform.

II. Wavelets And Wavelet Packet Approximation

The baseline wander elimination algorithm should be able to decompose the signal frequency components into precise levels to clearly distinguish between the signal and the wander, since there is fair amount overlap in the signal as well as the noise spectra in case of the bioimpedance signal. Wavelet decomposition can serve appropriate in this regard. A wavelet system is a set of building blocks from which one can construct or represent a signal or a function. It is a two-dimensional expansion set. The wavelet transform is a time-scale representation method that decomposes signal $x(t)$ into basis functions of time and scale which are dilated and translated versions of a basis function $\psi(t)$ which is called mother wavelet [11,12]. Equation 1 shows, how wavelets are generated from the mother wavelet.

$$\psi_{j,k}(t) = 2^{j/2} \psi(2^{j/2}t - k) \tag{1}$$

where j indicates the resolution level and k is the translation in time. This is called dyadic scaling, since the scaling factor is taken to be 2. Wavelet decomposition is a linear expansion and it is expressed as:

$$x(t) = \sum_{k=-\infty}^{\infty} c_k \phi(t - k) + \sum_{k=-\infty}^{\infty} \sum_{j=0}^{\infty} d_{j,k} \psi(2^j t - k) \tag{2}$$

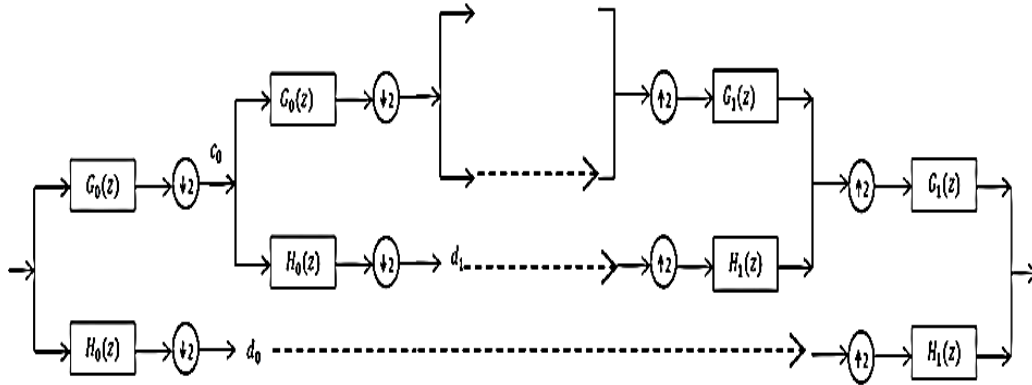


Figure 2. Filter bank representation of wavelet decomposition.

$$\psi(t) = \sum_k \sqrt{2}h_0(k)\phi(2t - k) \tag{3}$$

$$\phi(t) = \sum_k \sqrt{2}g_0(k)\phi(2t - k) \tag{4}$$

Here $G_0(z)$ and $H_0(z)$ are essentially low pass and high pass filters respectively, which split the signal bandwidth into half. To achieve the next level decomposition, the approximation coefficient is further passed this quadrature mirror filter bank formed by the low and high pass filters. These filters are related to wavelet $\psi(t)$ and scaling functions $\phi(t)$ as expressed in (3) and (4) [12]. The basic wavelet transform has only one-sided decomposition of the approximate coefficients. This is not sufficient in removal of noise sometimes. Hence to obtain more flexibility, the detail coefficient can also be decomposed in approximate and detail branches as shown in Fig. 3. This aids in exploring the other frequency band to correctly estimate the noise signal.

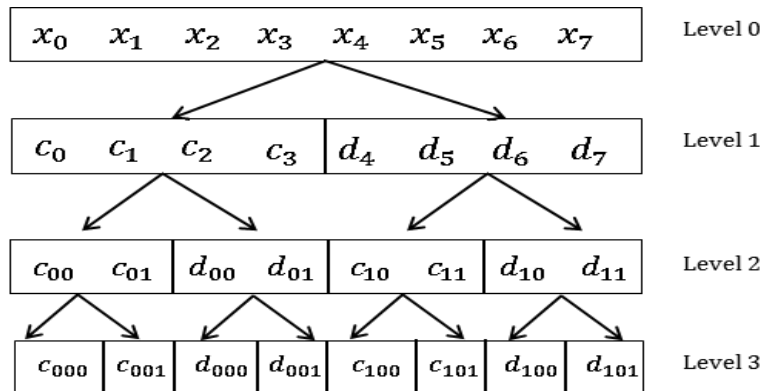


Figure 3. Wavelet Packet decomposition tree.

The algorithms for baseline wander removal using wavelet packet decomposition, proposed in this paper, is based on the assumption that the baseline drift signal is mixed with the bioimpedance signal in a linear fashion. Fig. 4 shows the flowchart for estimation and cancellation of the baseline wander. First, the wavelet packet decomposition of the bioimpedance signal is computed. The dyadic wavelet packet decomposition of the signal at a given level represents the projections of the signal on the basis functions of that level. To ensure that the representation is most accurate, the basis function should have higher resemblance with the signal variations. Initially the decomposition was carried out using the Daub-4 mother wavelet, Bior 2.8 and Symlet 4. The Daub-4 scaling function resembles the bioimpedance signal the most. The noise, SNR obtained using the Daub-4 is also better than the other two. The time of execution and thus the number of levels of decomposition were also found to be lesser in case of Daub-4. Thus the wavelet packet decomposition of the signal was done using Daub-4 wavelet. The energy of a signal is given in terms of the wavelet coefficients by Parseval’s relation as

$$\int |f(t)|^2 dt = \sum_{i=0}^{\infty} |c_i|^2 + \sum_{j=0}^{\infty} \sum_{k=-\infty}^{\infty} |d_{jk}|^2 \tag{5}$$

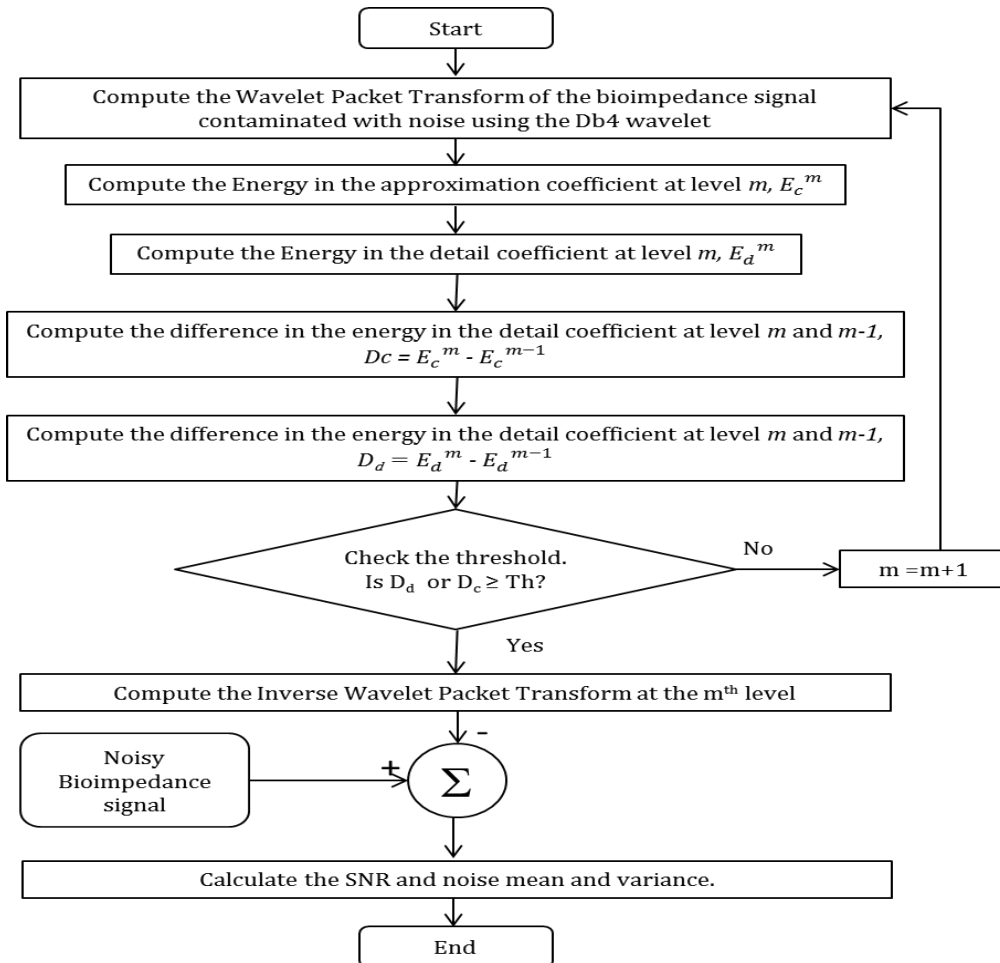


Fig. 4. Flowchart of bioimpedance baseline drift removal algorithm using wavelet packet transform.

At each step the energy of both, the approximation as well as the detail coefficients is calculated. The branch with the higher energy is decomposed further. This will be followed till the energy difference in the subsequent levels exceeds the preset threshold value. The algorithm adaptively computes the preset threshold for each signal. It was experimentally observed that whenever this value is between 0.7 % to 2% of the energy of the original signal, the last scale has been reached. Taking an average value of 1.0875% of the signal energy, gave acceptable results for all the subjects. The results obtained, using this method are discussed in the section IV.

III. Kalman Filter For Removal Of Baseline Drift

A good filtering algorithm should remove noise from the signal while retaining the useful information contained in it. One such filter, used in signal processing is the Kalman filter [13]. The Kalman filter is an efficient recursive filter that estimates the state of a linear dynamic system from a series of incomplete and noisy measurements. It is a tool that can estimate the variables of a wide range of processes. It defines a set of mathematical equations that provides an efficient computational (recursive) means to estimate the state of a process, in a way that minimizes the mean of the squared error. The filter is very powerful in several aspects: it supports estimations of present and even future states, and it can do so even when the precise nature of the modelled system is unknown. The Kalman filter has two distinct phases: Predict and Update. The predict phase uses the state estimate from the previous time step to produce an estimate of the state at the current time step. In the update phase, measurement information at the current time step is used to refine this prediction to arrive at a new, more accurate state estimate, again for the current time step. The Kalman filter not only works well in practice, but it is theoretically attractive because it can be shown that of all possible filters, it is the one that minimizes the variance of the estimation error. The proposed approach is used to identify and remove the baseline wandering in bioimpedance signals without adding any distortion to the signal. The Kalman filter approach is chosen because of its ability to simultaneously model both the bioimpedance signal and the baseline wandering. The algorithm implemented in this paper for removal of baseline wander is detailed below:

Algorithm for Kalman filter based baseline wander cancellation:

1. **Initial Prediction :**
 - a. Define a first order low pass filter with approximate cutoff frequency 0.8Hz. $\frac{0.0038}{1 - 0.9962z^{-1}}$
 - b. Pass the noisy signal through the filter to obtain the first noise estimate \hat{n} .
 - c. Define process noise covariance Q and measurement noise covariance R as $Q = \text{variance}(\hat{n})$ and $R = \text{variance}(\text{Noisy signal} - \hat{n})$.
2. **Initialization :**
 - a. Process Noise $w = 0$
 - b. Measurement noise $v = \text{variance}(\text{Noisy signal} - \hat{n})$
 - c. X_0 = the first sample of the noisy data
 - d. Error Covariance $P_0 = 100 * \text{variance}(\hat{n})$
 - e. $X_{k-1} = X_0$; $P_{k-1} = P_0$.
 - f. $H = 1$; State transition factor $A = [0.9962]$; Control input $B = [0.9962]$
3. **Measurement Update :**
 - a. Compute Kalman gain (K_k) : $K_k = P_{k-1}H^T(H P_{k-1}H^T + R)^{-1}$
 - b. Update estimate with measurement y_k
 $y_{k-1} = H X_{k-1} + v_k$
 $X_k = X_{k-1} + K_k(y_k - y_{k-1})$
 - c. Update the error covariance :
 $P_k = (I - K_k H) P_{k-1} (I - K_k H)^T + K_k R_k K_k^T$
4. **Time Update :**
 - a. Project the next state
 $X_{k-1} = A X_k + w$

IV. Simulation Results

In this section, the results obtained after applying the baseline wander algorithm using wavelet packet transform and the Kalman filter to different signals, are presented to illustrate the effectiveness of the algorithm. Table I details the various performance parameters such as noise mean, noise variance, improvement in SNR after noise removal, reduction in variance of the signal after noise removal and execution time obtained for different subjects using the wavelet packet transform based baseline removal algorithm. The similar results for the Kalman filter based baseline removal algorithm have been tabulated in Table II.

TABLE II: Performance Parameters of the Baseline Wander Removal Algorithm using Wavelet Packet Transform.

Subject	Noise mean	Noise variance	% Decrease in variance	SNRin (DB)	SNRout (DB)	SNR Rise %	Time for execution (sec)
Subject 1	73.75	57.90	76.57	-5.09	28.68	33.77	0.81
Subject 2	75.44	56.96	71.05	-3.65	29.35	33.00	0.84
Subject 3	76.00	68.47	87.61	-7.83	26.95	34.77	0.89
Subject 4	79.10	45.25	84.83	-6.57	26.40	32.97	0.75
Subject 5	76.88	249.82	94.46	-12.48	29.39	38.87	1.01

TABLE II: Performance Parameters of the Baseline Wander Removal Algorithm using Kalman Filter

Subject	Noise mean	Noise variance	% Decrease in variance	SNRin (DB)	SNRout (DB)	SNR Rise %	Time for execution (sec)
Subject 1	65.35	19.08	43.47	3.47	34.74	31.27	14.00
Subject 2	70.25	28.95	37.67	2.40	4.48	2.08	18.48
Subject 3	68.45	85.61	63.11	-4.66	10.02	14.68	18.35
Subject 4	72.92	34.19	42.46	-0.63	13.17	13.80	17.63
Subject 5	66.20	295.02	76.12	-6.76	35.41	42.16	9.22

The decrease in the variance is calculated as :

$$\% \text{ Decrease in variance} = \frac{\text{var}(\text{noisy signal}) - \text{var}(\text{clean signal})}{\text{var}(\text{noisy signal})} \times 100$$

The SNR improvement is computed in the following manner:

On the input side:

Calculate $\text{dbnoise} = 10 \cdot \log_{10}(\text{variance of noise signal})$

Calculate $\text{dbsignal} = 10 \cdot \log_{10}(\text{variance of clean signal})$

SNRin = $\text{dbsignal} - \text{dbnoise}$

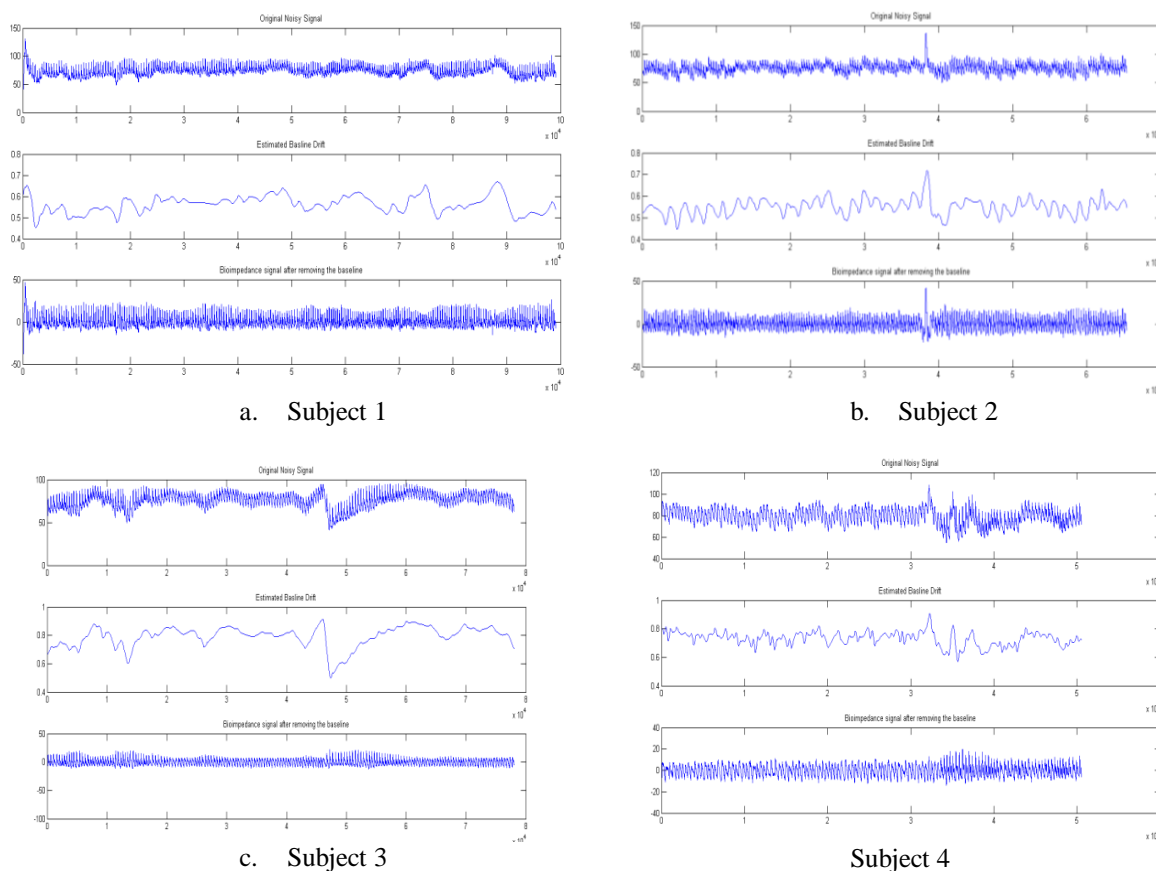
On the output side:

Y_1 = output of the filtering algorithm with the clean signal as input

Y_2 = output of the filtering algorithm with the noisy signal as input

SNRout = $10 \cdot \log_{10}(\text{variance of } Y_1) - 10 \cdot \log_{10}(\text{variance of } (Y_2 - Y_1))$

Fig. 5 and Fig.6 show the results of the baseline wander removal algorithm implemented on five subjects, using the wavelet packet transform and the Kalman filter, respectively. It can be concluded that the wavelet based algorithm is able to estimate the drift to a better extent than the Kalman filter. In case of Kalman filtering for canceling the artifacts, it is difficult to identify the filter parameters related to the sources of various artifacts. The time for execution in case of Kalman filter was also more as can be seen from Table. The improvement in the SNR is better in case of the wavelet packet transform. Form the results obtained in this paper, it can be said that the wavelet packet transform based adaptive algorithm implemented in this paper gives better results for elimination of baseline drift from the bioimpedance signals.



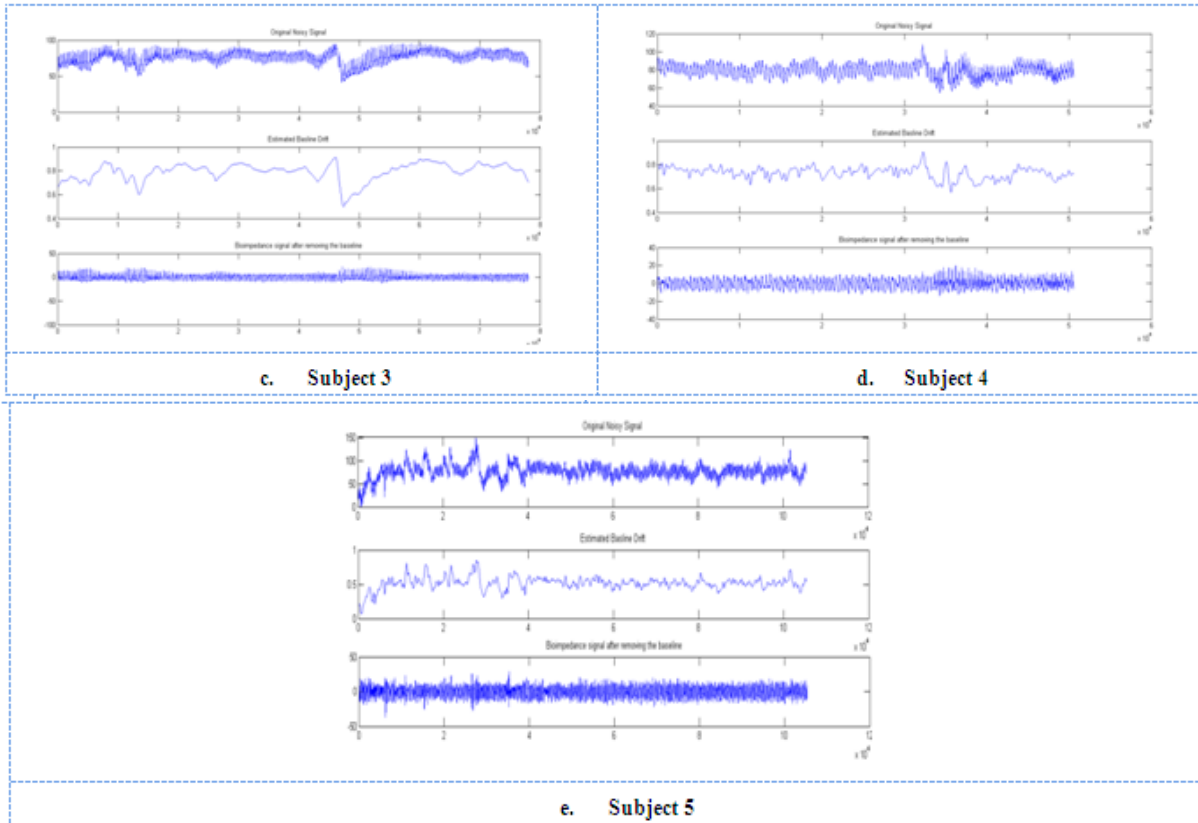
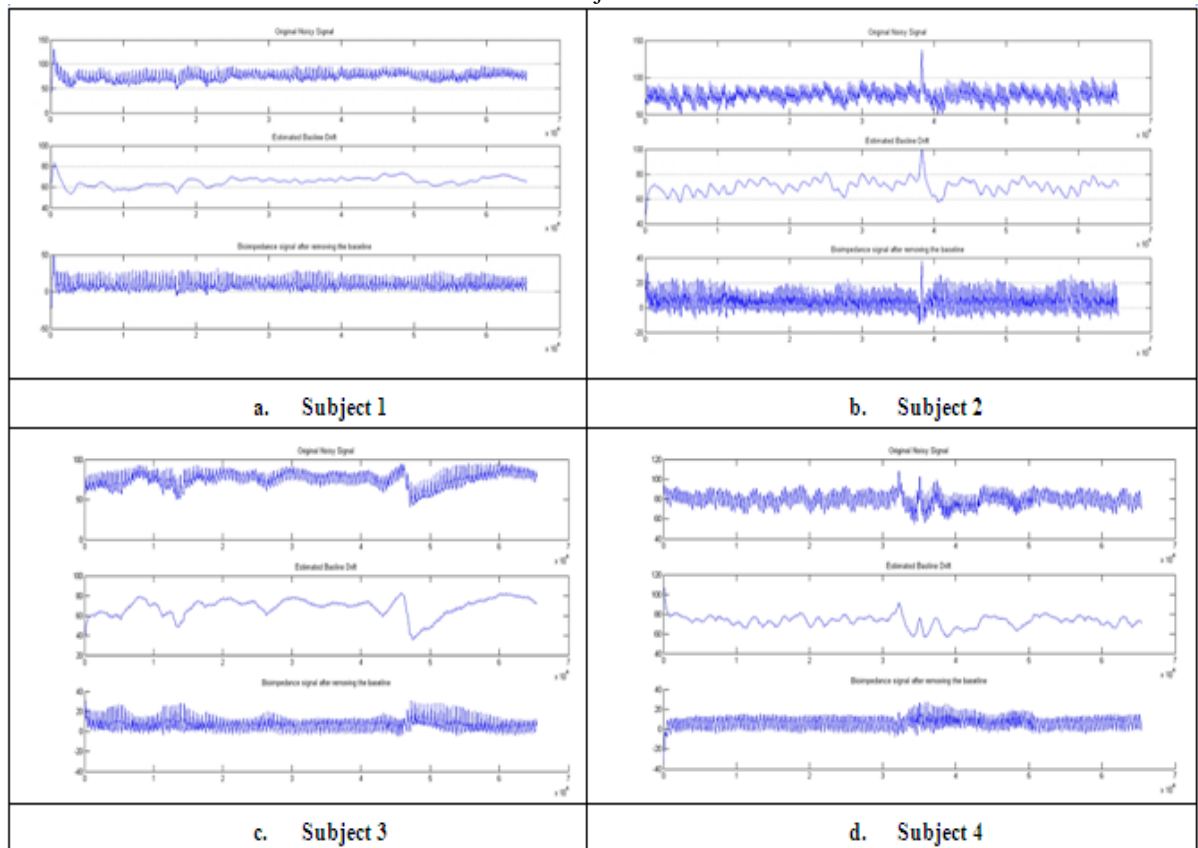
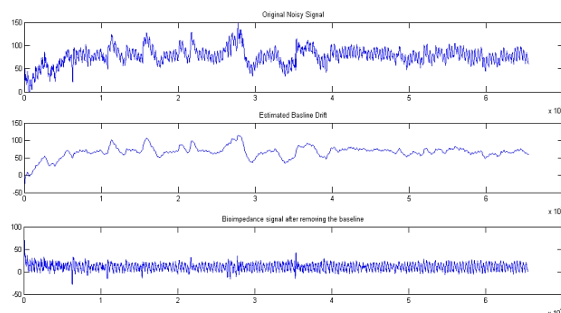


Figure 5. Filtered results obtained with wavelet packet based baseline wander removal algorithm for five subjects





e. Subject 5

Figure 6 Filtered results obtained with the Kalman filter based baseline wander removal algorithm for five subjects

V. Conclusion

The bioimpedance signal is of great importance in calculating the cardiac output, stroke volume and other cardiovascular parameters. It is of utmost importance to correctly locate the characteristic points on the signal, thereby producing error-free estimation of the parameters for diagnosis. Various baseline wander removal algorithms have been implemented in the literature for baseline drift cancellation, but most of them are applied to the ECG signals. The major challenge in baseline wander elimination from the bioimpedance signals was the spectral overlap between the noise and the signal. The amount of variations, obtained in the impedance at the wrist of the subject is very low as compared to the standard impedance cardiography signals which are measured along the human thorax. Since the signals were acquired at the wrist of the left hand, the original signal itself was weaker in amplitude. It was extremely important to preserve the energy and characteristic points of the signal after removal of the baseline drift.

The proposed adaptive wavelet packet based algorithm removes the baseline wander and preserve the clinical information of the bioimpedance records, without introducing any deformities in the signal. Since the number of levels of decomposition are calculated using the energy of the signal itself, each signal receives a different treatment for removal of the baseline drift. Eight to ten levels of dyadic wavelet packet decomposition were needed in each of the subject for correctly estimating the baseline drift. The Kalman filter based approach gives acceptable results in some subjects, but suffers from the problem of longer execution time, low SNR improvement. The use of extended Kalman filter instead of the traditional Kalman filter may help in improving the noise estimate thereby improving the SNR.

References

- [1] Vinod KP, Prem CP, Nitin JB, and Subramanyan LR. "Adaptive Filtering for Suppression of Respiratory Artifact in Impedance Cardiography", 33rd Annual International Conference of the IEEE EMBS: Boston, Massachusetts USA; August 30-September 3; 2011.
- [2] R. P. Patterson, "Fundamental of impedance cardiography," IEEE Eng. Med. Biol. Mag., vol. 8, pp. 35-38, Mar. 1989.
- [3] B. E. Hurwitz et al, "Coherent ensemble averaging techniques for impedance cardiography," in Proc.3rd Annu. IEEE Symp. Comp. Based Med. Syst., June 1988.
- [4] C. R. Meyer and H. N. Keiser, "Electrocardiogram baseline noise estimation and removal using cubic splines and statespace computation techniques," Computers and Biomedical Research, vol. 10, no. 5, pp. 459-470, 1977.
- [5] L. Sornmo, "Time-varying filtering for removal of baseline wander in exercise ECGs," in Proceedings of Computers in Cardiology, pp. 145-148, Venice, Italy, September 1991.
- [6] J. A. Van Alste and T. S. Schilder, "Removal of base-line wander and power-line interference from the ECG by an efficient FIR filter with a reduced number of taps," IEEE Transactions on Biomedical Engineering, vol. 32, no. 12, pp. 1052-1060, 1985.
- [7] I. I. Christov, I. A. Dotsinsky, and I. K. Daskalov, "High-pass filtering of ECG signals using QRS elimination," Medical and Biological Engineering and Computing, vol. 30, no. 2, pp. 253- 256, 1992.
- [8] Marquez JC, Rempfler M, Seoane F and Lindecrantz K. Textrode-enabled transthoracic electrical bioimpedance measurements-towards wearable applications of impedance cardiography. Journal of Electrical Bioimpedance: Vol. 4; pp. 45-50; 2013.
- [9] Piskulak P, Cybulski G, Niewiadomski W, and Paalko T. "Computer Program for Automatic Identification of Artifacts in Impedance Cardiography Signals Recorded during Ambulatory Hemodynamic Monitoring", XIII Mediterranean Conference on Medical and Biological Engineering and Computing 2013; IFMBE Proceedings 41, 2013
- [10] Gadre VM, Wavelets and Multirate Digital Signal Processing. Lecture 42: Application Assignment: Wavelet Based Denoising.
- [11] S. Mallat, A Wavelet Tour of Signal Processing, Academic Press, San Diego, Calif, USA, 2nd edition, 1999.
- [12] I. Daubechies, Ten Lecture on Wavelets, SIAM, Philadelphia, Pa, USA, 1992.
- [13] Haykin Simon, Adaptive Filer theory, Eaglewood Cliffs, New Jersey :Prentice- Hall, Inc, 1991.